AD_____

Award Number: W81XWH-09-1-0406

TITLE: Development of a Hybrid Optical Biopsy Probe to Improve Prostate Cancer Diagnosis

PRINCIPAL INVESTIGATOR: Hanli Liu

CONTRACTING ORGANIZATION: University of Texas at Arlington
Arlington, TX 76019

REPORT DATE: June 2012

TYPE OF REPORT: Annual

PREPARED FOR: U.S. Army Medical Research and Materiel Command
Fort Detrick, Maryland 21702-5012

REPORT DOCUMENTATION PAGE

Form Approved
OMB No. 0704-0188

1. REPORT DATE	2. REPORT TYPE	3. DATES COVERED
01-06-2012	Annual	1 JUN 2011 - 31 MAY 2012

4. TITLE AND SUBTITLE
Development of a Hybrid Optical Biopsy Probe to Improve Prostate Cancer Diagnosis

5a. CONTRACT NUMBER

5b. GRANT NUMBER
W81XWH-09-1-0406

5c. PROGRAM ELEMENT NUMBER

6. AUTHOR(S)
Hanli Liu

E-Mail: hanli@uta.edu

5d. PROJECT NUMBER

5e. TASK NUMBER

5f. WORK UNIT NUMBER

7. PERFORMING ORGANIZATION NAME(S) AND ADDRESS(ES)
University of Texas at Arlington
Arlington, TX 76019

8. PERFORMING ORGANIZATION REPORT NUMBER

9. SPONSORING / MONITORING AGENCY NAME(S) AND ADDRESS(ES)
U.S. Army Medical Research and Materiel Command
Fort Detrick, Maryland 21702-5012

10. SPONSOR/MONITOR'S ACRONYM(S)

11. SPONSOR/MONITOR'S REPORT NUMBER(S)

12. DISTRIBUTION / AVAILABILITY STATEMENT
Approved for Public Release; Distribution Unlimited

13. SUPPLEMENTARY NOTES

14. ABSTRACT
Hypothesis: a multi-modal optical spectroscopic method and an integrated needle probe can be developed for guiding needle biopsy for prostate cancer diagnosis. Multi-modal optical measurements to be utilized for the study are (1) light scattering spectroscopy (LSS), (2) auto-fluorescence spectroscopy (AFS), and (2) auto-fluorescence life-time measurements (AFLT). Our specific aims are:
Aim 1: to develop a multi-modal, optical spectroscopic instrument, which allows the measurements of (1) LSS, (2) AFS, and (3) AFLT. The proposed system will be portable, can be used for in vivo measurements, and collect and present the data in real time. Aim 2: to integrate the optical fibers, which collect light scattering and auto-fluorescence from the prostate tissue, into a transrectal-ultrasound, needle-biopsy probe. In the development phase, the optical signatures of prostate cancer can be collected with the biopsy tissues and identified along every tract of needle biopsies. Aim 3: to collect optical signals of control and cancer tissues ex vivo along with the regular human needle biopsy, followed by classification algorithm development to discriminate cancer tissues. Aim 4: to perform in vivo measurement from human subjects to obtain the accuracy and sensitivity of the integrated probe in order to provide real-time, on-site, improved guidance for prostate cancer tissue biopsy.

15. SUBJECT TERMS
Technology Development, optical spectroscopy, transrectal probe, optical biopsy, auto-fluorescence spectroscopy, fluorescence life-time measurement

16. SECURITY CLASSIFICATION OF:			17. LIMITATION OF ABSTRACT	18. NUMBER OF PAGES	19a. NAME OF RESPONSIBLE PERSON
a. REPORT	b. ABSTRACT	c. THIS PAGE			USAMRMC
U	U	U	UU	9	19b. TELEPHONE NUMBER *(include area code)*

Table of Contents

2011-2012 Annual Progress Report

This report presents the specific aims and accomplishments of our prostate cancer research project during the year of funding sponsored by the US Department of the Army. It covers our activities from May 2011-April 2012.

1. Introduction

The overall hypothesis for this study is that a multi-modal optical spectroscopic method and an integrated needle probe can be developed for guiding needle biopsy for prostate cancer diagnosis. Multi-modal optical measurements to be utilized for the study were (1) light reflectance spectroscopy (LRS), (2) auto-fluorescence spectroscopy (AFS), and (3) auto-fluorescence life-time measurements (AFLM).

The project has four specific aims:

Aim 1: to develop a multi-modal, optical spectroscopic instrument, which allows the measurements of (1) LRS, (2) AFS, and (3) AFLM. The proposed system will be portable, can be used for in vivo measurements, and collect and present the data in real time.

Aim 2: to integrate the optical fibers, which collect light scattering and auto-fluorescence from the prostate tissue, into a transrectal-ultrasound, needle-biopsy probe. In the development phase, the optical signatures of prostate cancer can be collected with the biopsy tissues and identified along every tract of needle biopsies.

Aim 3: to collect optical signals of control and cancer tissues ex vivo, followed by classification algorithm development to discriminate cancer tissues.

Aim 4: to perform in vivo measurement from human subjects to obtain the accuracy and sensitivity of the integrated probe in order to provide real-time, on-site, improved guidance for prostate cancer tissue biopsy.

2. Body of the Report

We completed Aim 1 in our Year 1 effort and reported it in Year 1 report. The 2nd year report summarized the work that we had performed in Year 2 from Sept. 1, 2010 to Dec. 31, 2011, mainly for Aim 2 and partially for Aim 3. This report will provide the information on our comprehensive effort to achieve Aim 3 in details and list corresponding achievements obtained during this period of time, as given below.

Aim 3: to collect optical signals of control and cancer tissues *ex vivo*, followed by classification algorithm development to discriminate cancer tissues.

In Year 2, we assembled an integrated unit for LRS and AFLM and tested them using laboratory tissue phantoms, followed by *ex vivo* measurements from several human prostate specimens after immediate removal from the patients. To accurately quantify cancer-specific signatures from both LRS and AFLM, we needed to perform comprehensive data analyses and to develop appropriate classification algorithms to discriminate cancer tissues, as described below.

2.1 Patients and sample size measured

The study was conducted as per the guidelines of Institutional Review Board at UT Southwestern Medical Center, Dallas, TX, and each patient's consent was obtained before the surgery. The study population was selected based on previous biopsy records and MRI (magnetic resonance imaging)

report. Selection criteria was high grade cancer (Gleason score ≥ 7), and high volume cancer (assessed by % involvement of the biopsy cores).

The sample size distribution is given in Table 1. A total of 29 prostate glands were measured. However, 6 samples showed 25% or less prostate cancer tissue (PCa) upon histopathology, and were excluded from analysis. Remaining 23 samples were used for data analysis. Some glands had multiple foci of PCa, resulting in 27 regions measured from 23 glands. Within each region, several (~8) optical readings were taken. Overall, 221 PCa locations were measured and categorized based on histopathology results into GS 7 (125), GS 8 (40) or GS 9 (56). Corresponding benign peripheral zone tissue (nPZ) and benign prostate hyperplasia (BPH) in each gland were also confirmed by histopathology and their distribution is also given in Table 1.

Table 1. Sample size distribution of this study. Top 2 rows represent the patients and region distribution by Gleason scores (GS), and bottom 3 rows represent the distribution of 539 measured locations by GS and tissue types.

	GS-7	GS-8	GS-9	Total
$N_{Subjects}$	13	4	6	**23**
$N_{Regions}$	15	5	7	**27**
N_{meas} **(PCa)**	125	40	56	**221**
N_{meas} **(nPZ)**	104	32	40	**176**
N_{meas} **(BPH)**	88	24	30	**142**

2.2 Data analysis for AFLM

Each lifetime curve was cropped to peak amplitude and normalized between 0 and 1. The resultant curve was then fitted to a conventional two-exponent model of lifetime decay [1], as shown in Eq. (1):

$$I(t) = a_1 e^{\tau_1} + a_2 e^{\tau_2} + c \,, \qquad (1)$$

where $I(t)$ represents normalized lifetime intensity, τ_1 and τ_2 are the lifetimes of the individual exponential components, and a_1 and a_2 are their respective weights. A constant term c was added to account for the baseline noise.

The data fitting was achieved through Matlab (The Mathworks, Inc., Natick, MA) by implementing a non-linear least squares curve fitting method. Also, intensity-weighted mean lifetime (τ_m) [2] was calculated, as given in Eq. (2):

$$\tau_m = (a_1\tau_1^2 + a_2\tau_2^2) / (a_1\tau_1 + a_2\tau_2) \,. \qquad (2)$$

Thus, five parameters of τ_1, τ_2, a_1, a_2 and τ_m were calculated for each of the four emission wavelengths (at 532 nm, 562 nm, 632 nm, 684 nm), giving us 20 parameters at each measured tissue location. Each of these parameters was further evaluated for significant differences among three types of prostate tissues: PCa versus two major benign prostate tissues, nPZ and BPH. We used a linear mixed model regression analysis for repeated measures, implemented in SAS software (SAS Institute Inc., NC, USA). Out of total 20 features, 16 features showed significant difference ($p<0.001$) for PCa vs nPZ and 19 features showed significant difference ($p<0.001$) when comparing PCa vs BPH.

As an example, Fig. 1 shows four of the AFLS features (i.e., mean-lifetime τ_m at all four wavelengths) that are significantly different between PCa versus nPZ and PCa sersus BPH. In the figure, the '*' above nPZ and BPH bars indicates significant difference ($p < 0.05$), when compared to PCa, and error bars indicate standard error of mean.

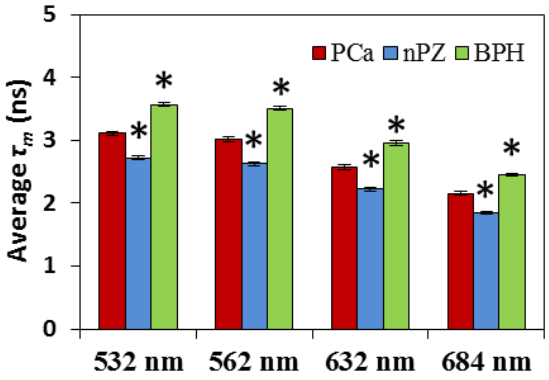

Figure 1

2.3 Data analysis for LRS

A spectral width of 500-850 nm was chosen; the corresponding data were fitted to a mathematical model (Eq. 3), details of which have been previously described in [3]. Briefly, in Eq. (3a), λ is the wavelength, R is the measured reflectance, μ_s' is the scattering coefficient, μ_a is the absorption coefficient, and k_1 & k_2 are empirically determined calibration constants.

$$R(\lambda) = \frac{\mu_s'(\lambda)}{k_1 + k_2 \mu_a(\lambda)} \qquad (3a)$$

$$\mu_a(\lambda) = \sum_{i=1}^{m} [c_i] \varepsilon_{c_i}(\lambda) \qquad (3b)$$

By using mathematical optimization algorithms, it is possible to derive μ_a and μ_s' values from Eq. (3a). The absorption coefficient, μ_a can be expressed as a sum of individual chromophore/absorber concentrations ([c]), weighted by their extinction coefficients (ε_c). The chromophores used in this model were deoxy-hemoglobin (Hb), oxy-hemoglobin (HbO), melanin (Mel), and β-carotene (β_{car}). The concentrations of all these chromophores ([Hb], [HbO], [Mel], [β_{car}]) were obtained for each measured location. Total hemoglobin concentration ([HbT] = [Hb] + [HbO]) was also calculated. Water concentration was assumed to be constant at 80%. Apart from tissue chormophores, we also measured the absorption spectra of the surface inking dyes, which were used routinely for histology marks, and included in the mathematical model to account for any residual dyes on the prostate tissue.

Scattering coefficient at 750 nm ($\mu_s'_{(750)}$), which is a parameter related to mean cell size and density in the measured region, was also obtained by fitting Eq. (3a). Thus, overall 6 parameters/features were extracted for each of 539 curves. These parameters were then analyzed for statistical differences between PCa and nPZ, as well as PCa and BPH, and p-values were obtained using a mixed model linear regression analysis model implemented in SAS (SAS Institute Inc., NC, USA). When comparing PCa vs nPZ, all LRS parameters except *[Mel]* showed significant difference ($p < 0.001$), whereas for PCa vs BPH, [Hb], [β_{car}], and $\mu_s'_{(750)}$ were found to be significantly ($p < 0.02$) different (see Fig. 2). Note that light scattering was much higher in cancer tissue as compared to other two benign prostate tissue types, and hemoglobin concentrations were lower in PCa than in nPZ. Also, [β_{car}] in PCa was higher than BPH tissue, but lower than nPZ. Similarly to Fig. 1, the '*' above nPZ and BPH bars indicates significant difference ($p < 0.05$), when compared to PCa, and error bars indicate standard error of mean.

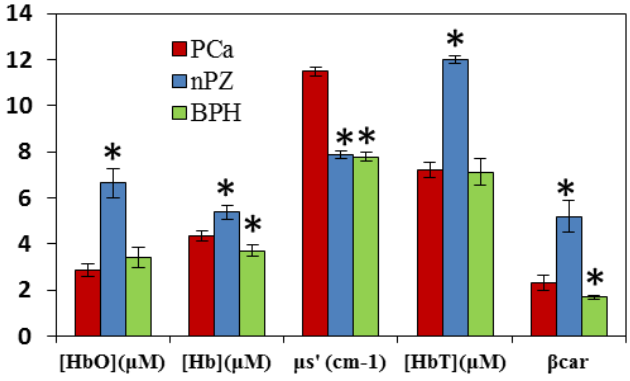

Figure 2

2.4 Data classification and accuracy assessment

To test the ability to differentiate cancer from benign tissue, two types of algorithms were implemented. First, we tested the ability to differentiate prostate cancer (PCa, all grades combined), from two benign tissue types (nPZ, BPH) in a 3-way classification algorithm. Next, we evaluated the ability to further differentiate different grades of PCa (i.e. GS 7, GS 8, and GS 9), in a 5-way classification algorithm. Above two algorithms were evaluated independently for all three methods, namely, LRS, AFLS, and *dual modality* (LRS + AFLS combined).

The classification was achieved through a multinomial logistic regression (MLR) model with 10-fold cross validation, implemented in Matlab (The Mathworks, Inc., Natick, MA). The detailed description of our MLR model has been described previously [4]. Briefly, first, a set of optimum parameters from a given set of parameters (6 for LRS, 20 for AFLS, and 26 for *the combined method*) were selected so that they could provide the best classification ability. This step served to remove the redundant features and improve classification accuracy, as well as to avoid over-fitting in the MLR model.

Next, the selected parameters were used in an MLR model, which was implemented with 10-fold cross validation [4]. In 10-fold cross validation, the entire data set (539 observations) was first divided into training set (90% of data) and test set (10% of data). The MLR model was built using the training data, and classification metrics are calculated on the test set, which was not included during model building. We calculated *sensitivity*, *specificity*, *accuracy*, and *receiver operating curves* (ROC) on the test set as the metrics for classification. This procedure was repeated 10 times by selecting different test and training sets each time, thus randomly covering the entire data set. The metrics were further averaged across the 10 test sets. Moreover, the 10-fold cross validation procedure described above was executed 10 times, to obtain a mean and standard deviation of the classification metrics.

Although looking at individual means gives an intuition about fundamental differences in the tissue types, our main goal is to differentiate PCa from non-cancer (nPZ and BPH) prostate tissues. This was achieved by selecting the best parameter set, and using them to classify different tissue types. Table 2 shows results for differentiating PCa (all grades combined) against benign prostate tissue types using LRS or AFLS individually, as well in a combined approach (LRS+AFLS). All the classification metrics indicate better values for *the combined method* as compared to either of the individual mode.

Table 2. Classification metrics of PCa (all types combined) against non-cancer tissue types (nPZ and BPH).

Mode	Sensitivity	Specificity	Accuracy	AUC
AFLM	64.2 ± 2.5	69.2 ± 1.8	67.1 ± 0.7	72.9 ± 0.5
LRS	63.0 ± 1.5	82.9 ± 1.6	74.7 ± 1.0	80.4 ± 0.2
combined	79.0 ± 1.7	85.2 ± 1.1	**82.7 ± 0.7**	**90.8 ± 0.4**

Furthermore, classification metrics for different grade of PCa by Gleason score (GS) was also obtained. The results are listed in Table 3. Once again, *the combined modality* shows better accuracy and AUC as compared to each modality individually used for all three Gleason scores.

Table 3. Classification metrics of PCa categorized by Gleason scores. The values listed implicate classification of the respective tissue type (GS) against rest of the tissue types.

PCa Type	Mode	Sensitivity	Specificity	Accuracy	AUC
GS 9	*LRS*	84.4 ± 2.3	56.5 ± 0.7	59.4 ± 0.6	72.9 ± 0.5
	AFLM	76.5 ± 3.2	75.9 ± 1.0	76.0 ± 0.9	85.4 ± 0.6
	dMOD	82.3 ± 2.4	85.4 ± 0.7	**85.1 ± 0.6**	**91.5 ± 0.7**
GS 8	*LRS*	71.8 ± 2.6	72.6 ± 1.8	72.5 ± 1.6	77.1 ± 0.7
	AFLM	76.3 ± 4.9	86.7 ± 0.8	86.0 ± 0.6	90.0 ± 0.6
	dMOD	81.5 ± 3.4	90.8 ± 0.9	**90.1 ± 0.8**	**93.6 ± 0.7**
GS 7	*LRS*	71.9 ± 2.2	82.7 ± 1.3	80.2 ± 0.7	87.9 ± 0.2
	AFLM	70.9 ± 2.0	72.4 ± 0.9	72.1 ± 0.7	78.6 ± 0.7
	dMOD	86.0 ± 2.4	88.5 ± 0.7	**87.9 ± 0.6**	**94.7 ± 0.4**

3. Key Research Accomplishments and Reportable Outcomes

(1) We have performed *ex vivo* measurements taken from human prostate specimens using the newly implemented and integrated dual-modality optical system, with a large sample size, n=23, covering Gleason scores from 7 to 9.

(2) We have quantitatively analyzed both LRS and AFLM signals from the human prostate specimens, using mixed model analysis; we have found significant differences in multiple optical parameters derived from LRS and AFLM.

(3) We have developed and utilized a multinomial logistic regression method for discrimination of prostate cancer tissues from benign prostate tissues (i.e. nPZ, BPH). We have also demonstrated that best classification was achieved with dual-modality approach, as opposed to either modality alone.

(4) We can successfully classify prostate cancer tissues with an accuracy of 82% when comparing benign prostate tissues. Further, we are able to identify different levels of cancer aggressiveness by classifying GS9, GS8, and GS7 with accuracy of 85.1%, 90.1%, and 87.9%, respectively.

(5) Several related research works are presented and/or submitted to peer-reviewed journals:

(a) Ronak H. Patel, Aniket S. Wadajkar, Nimit L. Patel, Venkaiah C. Kavuri, Kytai T. Nguyen, Hanli Liu*, "Multifunctionality of indocyanine green-loaded biodegradable nanoparticles for enhanced optical imaging and hyperthermia intervention of cancer," *J. Biomed. Opt.* 17(4), 046003 (2012).

(b) Vikrant Sharma, Payal Kapur, Ephrem Olweny, Jeffrey Cadeddu, Claus R Roehrborn, and Hanli Liu*, "Auto-fluorescence lifetime spectroscopy for prostate cancer detection: *An optical biopsy approach*," to be submitted to *European Urology* (2012).

(c) Vikrant Sharma, Payal Kapur, Ephrem Olweny, Jeffrey Cadeddu, Claus R Roehrborn, and Hanli Liu, "Auto-fluorescence lifetime spectroscopy for prostate cancer detection: An optical biopsy approach," accepted for presentation at *OSA Optics Photonics Congress*, Miami, Florida, April 29-May 3, 2012.

(d) Vikrant Sharma, Nimit Patel, and Hanli Liu, "Optical Biopsy using light reflectance spectroscopy for Prostate cancer diagnosis," *SPIE, Photonics West*, BiOS Biomedical Optics Symposium, oral presentation, paper 7883B-42, Jan. 23-26, 2011, San Francisco, California.

4. Conclusions and plan for the extended year

In summary, for the report period from May 2011 to April 2012, we can conclude that auto-fluorescence lifetime decay of prostate cancer tissue with excitation at 447 nm and emission in range of 532 nm to 684 nm shows significant contrast when compared with surrounding benign prostate tissue. This new technique shows a great promise, and further studies with a larger sample size are warranted to assess the technique *in vivo*. Specifically, in the coming year, we will carry on the development for Aim 4.

5. References:

1. J. Siegel, D. S. Elson, S. E. D. Webb, K. C. B. Lee, A. Vlanclas, G. L. Gambaruto, S. Leveque-Fort, M. J. Lever, P. J. Tadrous, G. W. H. Stamp, A. L. Wallace, A. Sandison, T. F. Watson, F. Alvarez and P. M. W. French, "Studying biological tissue with fluorescence lifetime imaging: microscopy, endoscopy, and complex decay profiles," Applied Optics **42**, 2995-3004 (2003).
2. C. W. Chang, D. Sud and M. A. Mycek, "Fluorescence lifetime imaging microscopy," Methods Cell Biol **81**, 495-524 (2007).
3. V. Sharma, J.W. He, S. Narvenkar, Y.B. Peng, H. Liu, "Quantification of light reflectance spectroscopy and its application: determination of hemodynamics on the rat spinal cord and brain induced by electrical stimulation," Neuroimage **56**(3), 1316-28 (2011).
4. V. Sharma, S. Shivalingaiah, Y. Peng, D. Euhus, Z. Gryczynski, and H. Liu, "Auto-fluorescence lifetime and light reflectance spectroscopy for breast cancer diagnosis: *potential tools for intra-operative margin detection,"* Biomedical Optics Express, to be published (2012).